Steel and Composite Structures, Vol. 2, No. 4 (2002) 237-246
DOI: http://dx.doi.org/10.12989/scs.2002.2.4.237

Stress fields on an isotropic semi-infinite plane with a circular hole subjected to arbitrary loads using the constraint-release technique

Takashi Tsutsumi†

Department of Civil Engineering, Kagoshima National College of Technology, Hayato, Kagoshima, 899-5193, Japan

Keiji Sato‡

Department of Civil Engineering, Oita Technical High School, Oita, 870-0948, Japan

Ken-ichi Hirashima‡†

Department of Civil and Environmental Engineering, Yamanashi University, Kofu, Yamanashi, 400-8511, Japan

Hiroshi Arai‡‡

Department of General Education, Fukushima National College of Technology Iwaki, Fukushima, 970-8034, Japan

(Received September 17, 2001, Revised June 3, Accepted July 15, 2002)

Abstract. In this paper, the solution of a semi-infinite plane with one circular hole is presented. This solution is induced by repeatedly superposing the solution of an infinite plane with one circular hole and that of a semi-infinite plane without holes to cancel out the stresses arising on both boundaries. This procedure is carried out until the stresses arising on both boundaries converge. This method does not require complicated calculation procedures as does the method using stress functions defined in a bipolar coordinate system. Some numerical results are shown by graphical representations.

Key words: shallow circular hole; arbitrary load; stress analysis; constraint-release technique.

1. Introduction

The problem of a semi-infinite plane with one circular hole is very important for the strength of materials or driving tunnels. Solutions for this have been induced using stress functions on a bipolar

†Associate Professor, D. Eng.
‡Instructor, D. Eng.
‡†Professor, D. Eng.
‡‡Associate Professor, M. Sc.

coordinate system Jeffery (1920), Mindlin (1939), Verruijt (1997b) or using the Finite Element Method.

However, analyses which use stress functions on a bipolar coordinate system have the following drawbacks: First, the procedure for obtaining solutions to isotropic problems is inevitably complicated. Second, for orthotropic problems, there is no mapping function which simultaneously maps the two boundaries into concentric circles. In addition, these studies treat only the case that is under axial symmetry load on a circular hole. Analyses which use the FEM have the following drawbacks: First, the calculations consume a huge amount of computer memory resources. Second, the accuracy of the solution depends on the method by which the problem is meshed.

On the other hand, solutions have been induced for doubly connected elastic problems by superposing the two kinds of elastic solution for simply connected problems until stresses on both boundaries converge to the boundary conditions Howland (1930), Tamate (1957b) (1959), Hetenyi (1960), Tsutsumi, *et al*. (1997a), (2000). This procedure allows us to obtain the final solution for doubly connected elastic problems.

In this paper, this method is called the Constraint-Release Technique, and has been used to verify the solution to the problem of an semi-infinite plane with one circular hole under arbitrary load on a circular hole.

2. Fundamental equations

Consider a two-dimensional semi-infinite plane with one circular hole, as presented in Fig. 1. The stress components σ_x, σ_y and τ_{xy} and displacement components u_x and u_y are represented by the following equations:

$$\left.\begin{aligned} \sigma_x &= 2Re[\varphi'(z)] - Re[\bar{z}\varphi''(z) + \psi''(z)] \\ \sigma_y &= 2Re[\varphi'(z)] + Re[\bar{z}\varphi''(z) + \psi''(z)] \\ \tau_{xy} &= Im[\bar{z}\varphi''(z) + \psi''(z)] \end{aligned}\right\} \tag{1}$$

$$u_x - iu_y = \frac{1}{2G}[\kappa\overline{\varphi(z)} - \{\bar{z}\varphi'(z) + \psi'(z)\}] \tag{2}$$

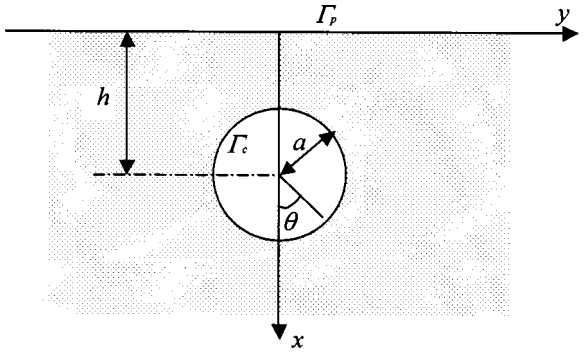

Fig. 1 Semi-infinite plane with one circular hole

$$\kappa = \begin{cases} \dfrac{3-\nu}{1+\nu} & :plane\ stress \\ 3-4\nu & :plane\ stress \end{cases} \tag{3}$$

where $z = x + iy$, i is the imaginary unit; $\varphi(z)$ and $\psi(z)$ are the stress functions introduced by Kolosov and Muskhelishvili; *Re* and *Im* denote the real part and the imaginary part of the complex functions, and ν and G represent the Poisson ratio and shear modulus, respectively.

The formulae which map stress and displacement components into curvilinear coordinates (ξ, η) are given by

$$\left.\begin{aligned} \sigma_\xi + \sigma_\eta &= \sigma_x + \sigma_y \\ \sigma_\eta - \sigma_\xi + 2i\tau_{\xi\eta} &= e^{2i\theta}(\sigma_y - \sigma_x + 2i\tau_{xy}) \end{aligned}\right\} \tag{4}$$

$$u_\xi - iu_\eta = e^{i\theta}(u_x - iu_y) \tag{5}$$

3. Formulation of the problem

The purpose of this paper is to obtain the solution for a problem in which an arbitrary load is applied to the only circular hole of a semi-infinite plane. We obtain the solution for this problem by the following procedure. First, the tangential stress $\sigma^c_{\xi,0}$ and shear stress, $\tau^c_{\xi\eta,0}$, on the circular hole are expanded in finite Fourier expansions,

$$\sigma^c_{\xi,0} - i\tau^c_{\xi\eta,0} = \bar{c}_{0,0} + \sum_{m=1}^{M} (\bar{c}_{0,m}\cos m\theta + \bar{d}_{0,m}\sin m\theta) \tag{6}$$

The stress functions for an infinite plane with one circular hole, as shown in Fig. 2, are given by

$$\left.\begin{aligned} \varphi_{c,0}(z) &= M_0 \log(z-h) + \sum_{m=1}^{M} A_{0,-m}(z-h)^{-m} \\ \psi_{c,0}(z) &= N_0(z-h)\log(z-h) + K_0 \log(z-h) + \sum_{m=1}^{M} B_{0,-m}(z-h)^{-m} \end{aligned}\right\} \tag{7}$$

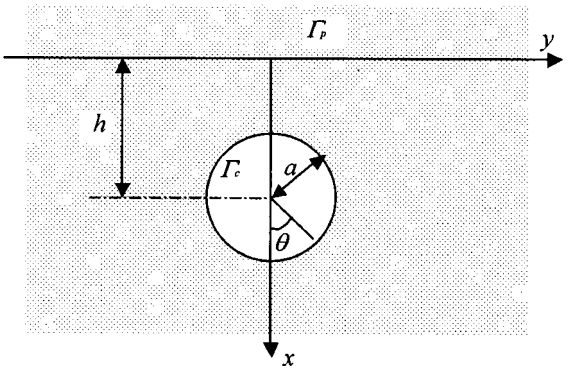

Fig. 2 Infinite plane with one circular hole

The complex coefficients M_0, N_0, K_0, $A_{0,-m}$, $B_{0,-m}$ are obtained as in the following form:

$$\left.\begin{aligned} M_0 &= \frac{1-\nu}{8}(c_{0,1}+id_{0,1}) \\ N_0 &= \frac{3-\nu}{8}(\bar{c}_{0,1}-i\bar{d}_{0,1}) \\ K_0 &= \bar{c}_{0,0}a^2 \\ A_{0,-m} &= -\frac{a^{m+1}}{m}\frac{c_{0,m+1}+id_{0,m+1}}{2} \quad m\geq 1 \\ B_{0,-1} &= \frac{a^3}{2}\left(\frac{1+\nu}{2}\frac{c_{0,1}+id_{0,1}}{2}-\frac{\bar{c}_{0,1}+i\bar{d}_{0,1}}{2}\right) \\ B_{0,-m} &= \frac{a^{m+2}}{m}\left(\frac{c_{0,m}+id_{0,m}}{2}-\frac{c_{0,m}+id_{0,m}}{2(m+1)}\right) m\geq 2 \end{aligned}\right\} \tag{8}$$

The tangential stress $\sigma^*_{x,0}$ and the shear stress $\tau^*_{xy,0}$ on the virtual straight boundary ($x = 0$) are represented using the stress functions:

$$\left.\begin{aligned} \sigma^*_{x,0} &= 2Re[\varphi'_{c,0}(z)]-Re[\bar{z}\varphi''_{c,0}(z)+\psi''_{c,0}(z)] \\ \tau^*_{xy,0} &= Im[\bar{z}\varphi''_{c,0}(z)+\psi''_{c,0}(z)] \end{aligned}\right\} \tag{9}$$

The terms in the above equations are expanded as in the following equations, where $F_{0,n}$, $\hat{F}_{0,n}$, $H_{0,n}$, $\hat{H}_{0,n}$, $H^*_{0,n}$, $\hat{H}^*_{0,n}$, $J_{0,n}$, $\hat{J}_{0,n}$, $J^*_{0,n}$, $\hat{J}^*_{0,n}$, are complex coefficients which are determined by M_0, N_0, K_0, $A_{0,-m}$, and $B_{0,-m}$.

$$\left.\begin{aligned} Re[\varphi'_{c,0}(z)] &= \sum_{k=1}^{K}\frac{F_{0,k}}{(y^2+h^2)^k}+\sum_{k=1}^{K}\frac{y\hat{F}_{0,k}}{(y^2+h^2)^k} \\ Re[\bar{z}\varphi''_{c,0}(z)] &= \sum_{k=1}^{K}\frac{H_{0,k}}{(y^2+h^2)^k}+\sum_{k=1}^{K}\frac{y\hat{H}_{0,k}}{(y^2+h^2)^k} \\ Im[\bar{z}\varphi''_{c,0}(z)] &= \sum_{k=1}^{K}\frac{yH^*_{0,k}}{(y^2+h^2)^k}+\sum_{k=1}^{K}\frac{\hat{H}^*_{0,k}}{(y^2+h^2)^k} \\ Re[\psi''_{c,0}(z)] &= \sum_{k=1}^{K}\frac{J_{0,k}}{(y^2+h^2)^k}+\sum_{k=1}^{K}\frac{y\hat{J}_{0,k}}{(y^2+h^2)^k} \\ Im[\psi''_{c,0}(z)] &= \sum_{k=1}^{K}\frac{yJ^*_{0,k}}{(y^2+h^2)^k}+\sum_{k=1}^{K}\frac{\hat{J}^*_{0,k}}{(y^2+h^2)^k} \end{aligned}\right\} \tag{10}$$

K in Eq. (10) and M in Eq. (7) do not have to be same because the terms in Eq. (10) are obtained by Fourier integral. Therefore, $\sigma^*_{x,0}$ and $\tau^*_{xy,0}$ are represented as:

$$\sigma^*_{x,0} = \sum_{k=1}^{K}\left\{\tilde{\sigma}^{\bullet}_{x,k}\frac{1}{(y^2+h^2)^k} + \tilde{\sigma}'_{x,k}\frac{y}{(y^2+h^2)^k}\right\}, \quad \tau^*_{xy,0} = \sum_{k=1}^{K}\left\{\tilde{\tau}^{\bullet}_{x,k}\frac{1}{(y^2+h^2)^k} + \tilde{\tau}'_{x,k}\frac{y}{(y^2+h^2)^k}\right\} \tag{11}$$

where

$$\begin{aligned} \tilde{\sigma}^{\bullet}_{x,k} &= 2F_{0,k} - H_{0,k} - J_{0,k}, & \tilde{\sigma}'_{y,k} &= 2\hat{F}_{0,k} - \hat{H}_{0,k} - \hat{J}_{0,k} \\ \tilde{\tau}^{\bullet}_{xy,k} &= H^*_{0,k} + J^*_{0,k}, & \tilde{\tau}'_{xy,k} &= \hat{H}^*_{0,k} + \hat{J}^*_{0,k} \end{aligned} \tag{12}$$

Then, in order to cancel out the stresses represented in Eq. (9), the negative values of these stresses are loaded on the semi-infinite plane. The stress functions for a semi-infinite plane are represented as:

$$\left.\begin{aligned} \varphi'_{p,1}(z) &= \frac{a_1(0)}{2}\frac{1}{z} + \int_0^{\infty} e^{-zt}\,\frac{a_1(t) - a_1(0) + ib_1(t)}{2}dt \\ \psi''_{p,1}(z) &= \frac{\overline{a_1(0)}}{2}\frac{1}{z} + \int_0^{\infty} e^{-zt}\left\{\frac{\overline{a_1(t)} - \overline{a_1(0)} + \overline{ib_1(t)}}{2} + \frac{a_1(t) + ib_1(t)}{2} + zt\frac{a_1(t) + ib_1(t)}{2}\right\}dt \end{aligned}\right\} \tag{13}$$

where

$$\left.\begin{aligned} a_1(0) &= -\frac{1}{\pi}(P_{y,1} + iP_{x,1}) \\ a_1(t) &= -\frac{2}{\pi}\int_0^{\infty}[\sigma^*_{x,0} + i\tau^*_{xy,0}]\cos(ty)dy, \quad b_1(t) = -\frac{2}{\pi}\int_0^{\infty}[\sigma^*_{x,0} + i\tau^*_{xy,0}]\sin(ty)dy \end{aligned}\right\} \tag{14}$$

In the above equations, $P_{y,1}$ and $P_{x,1}$ are the resultant forces in the x-direction and y-direction, respectively. Furthermore, $a_1(t)$ and $b_1(t)$ are expanded as the following series:

$$a_1(t) = \sum_{k=1}^{K}\tilde{a}_{1,k}\ t^{k-1}e^{-th}, \quad b_1(z) = \sum_{k=1}^{K}\tilde{b}_{1,k}\ t^{k-1}e^{-th} \tag{15}$$

By using the above equations and the Laplace transformation, Eqs. (13) may be represented as follows:

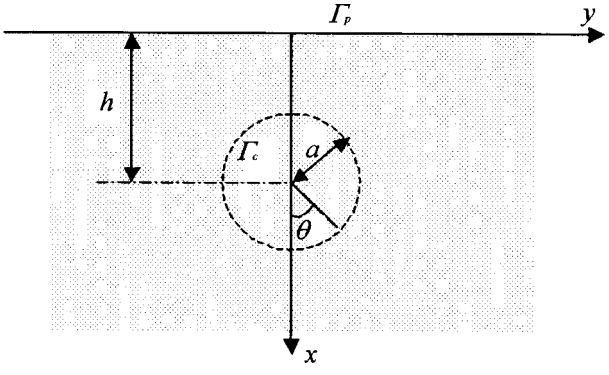

Fig. 3 Semi-infinite plane without holes

$$\varphi'_{p,1}(z) = \sum_{k=1}^{K} \frac{(k-1)!(\tilde{a}_{1,k} - \tilde{b}_{1,k})}{2(z+h)^k}, \quad \psi''_{p,1}(z) = -\sum_{k=1}^{K} \left\{ \frac{(k-1)!\tilde{b}_{1,k}}{(z+h)^k} + \frac{k!(\tilde{a}_{1,k} - \tilde{b}_{1,k})z}{2(z+h)^{k+1}} \right\} \tag{16}$$

On using these stress functions, the tangential stress, $\sigma_{\xi,1}$, and the shear stress, $\tau_{\xi\eta,1}$, arising on the virtual circular hole boundary in the semi-infinite plane without holes are represented as:

$$\sigma_{\xi,1} - i\tau_{\xi\eta,1} = \bar{c}_{1,0} + \sum_{m=1}^{M} (\bar{c}_{1,m}\cos m\theta + \bar{d}_{1,m}\sin m\theta) \tag{17}$$

For cancelling out these stresses, the negative values of the stresses represented in Eq. (17) are again loaded on the boundary of the circular hole of the infinite. By repeating this procedure, the stress functions for the semi-infinite plane with one circular hole are obtained using the following equations:

$$\varphi(z) = \sum_{n=0}^{N} \varphi_{c,n}(z) + \sum_{n=1}^{N} \varphi_{p,n}(z), \quad \psi(z) = \sum_{n=0}^{N} \psi_{c,n}(z) + \sum_{n=1}^{N} \psi_{p,n}(z) \tag{18}$$

where

$$\left.\begin{aligned}
\varphi_{c,n}(z) &= M_n \log(z-h) + \sum_{m=1}^{m} A_{n,-m}(z-h)^{-m} \\
\psi_{c,n}(z) &= N_n(z-h)\log(z-h) + K_n \log(z-h) + \sum_{m=1}^{M} B_{n,-m}(z-h)^{-m} \\
\varphi_{p,n}(z) &= \frac{a_n(0)}{2}\log z - \int_0^\infty e^{-zt}\frac{a_n(t) - a_n(0) + ib(t)}{2t}dt \\
\psi_{p,n}(z) &= -\frac{\overline{a_n(0)}}{2}\log z + \int_0^\infty e^{-zt}\left\{ -\frac{\overline{a_n(t)} - \overline{a_n(0)} + \overline{ib_n(t)}}{2t} - z\frac{a_n(t) + ib_n(t)}{2} \right\}dt
\end{aligned}\right\} \tag{19}$$

In Eq. (19), $\log(z-h)$ and $\log z$ are many-valued. However, the first differential and second differential of $\varphi_{c,n}(z)$ and $\varphi_{p,n}(z)$, and the second differential of second differential of $\psi_{c,n}(z)$ and $\psi_{p,n}(z)$, are used to obtain the stresses as shown in Eq. (1), so that the terms involving $\log(z-h)$ or $\log z$ are reduced to be single valued.

4. Results and discussion

To investigate the convergence of the stresses arising on the circular hole, Fig. 5 shows the stresses arising on the boundary of the hole under uniform normal stress on the hole boundary as shown in Fig. 4. In this graph, the transverse axis shows the angle from the bottom of the circular hole, and the ordinate axis shows normal stress arising on the hole. The graph shows the results when the ratio of the distance between the straight boundary and the center of the hole, h, to the radius of the circular hole a is 1.5 and 5.0, and the number of calculation repetitions N that is shown in Eqs. (18) is 3, 6 and 9 when h/a = 1.5, and 1, 2 and 3 when h/a = 5.0. In general, the stress on the hole boundary decreases as the number of calculation repetitions increases. Convergence of the stress arising on the boundary comes

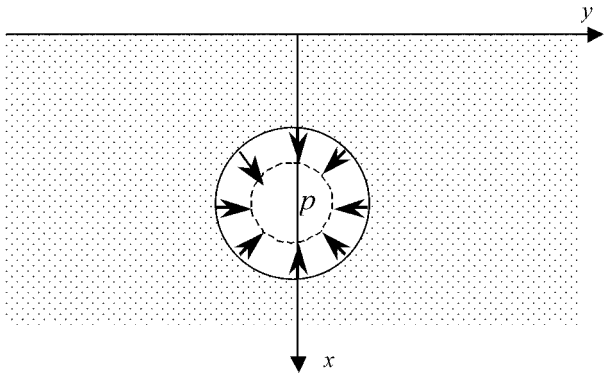

Fig. 4 Uniform normal stress on the hole

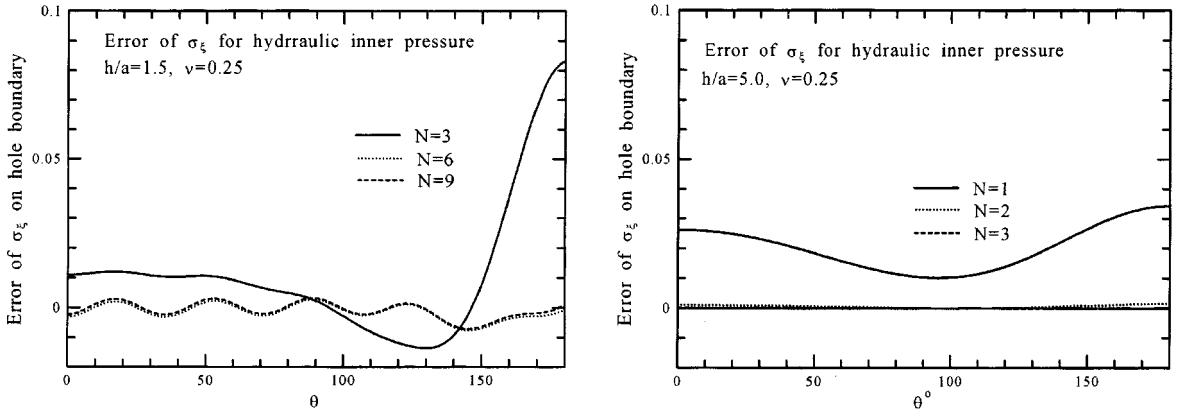

(a) h/a=1.5 (b) h/a=5.0

Fig. 5 Error on the hole boundary

more rapidly as the ratio h/a increases. When the hole is deep (i.e., h/a = 5.0), the error on the boundary is about 3.5% for N = 1 and N = 3 is enough to calculate the stresses. On the other hand, when the hole is shallow (i.e., h/a = 2.0), the convergence is in comparison with the case when the hole is deep. Nevertheless, 6 repetitions of the calculation are enough to retrieve the stresses when h/a = 1.5. Fig. 6 shows the stresses arising on the straight boundary when N = 9. In this graph, the transverse axis shows the ratio of the distance from the point above the center of the hole y to the radius of hole a, and the ordinate axis shows the ratio of the normal stress σ_x arising on the straight boundary to the magnitude of uniform normal stress p acting on the hole boundary. The normal stress remains above the center of hole, and becomes greater as h/a increases. However, it appears that this method provides adequate accuracy when h/a is greater than 1.8 because σ_x / p is then less than 5%.

Fig. 7 shows the tangential stress around the circular hole at h/a = 2.0 and 5.0 when a uniform normal stress p is loaded on the circular hole as shown in Fig. 4. When the hole is deep, uniform compression appears around the hole. However, it should be noted that the tangential stress around the hole is influenced by the straight boundary when the hole is shallow (i.e., h/a = 2.0).

Fig. 9 shows the tangential stress around the circular hole at h/a = 2.0 and 5.0 when symmetric stress that depends on the polar angle, namely on θ, $\sigma_\xi = p \cos 2\theta$, is loaded on the circular hole as shown in

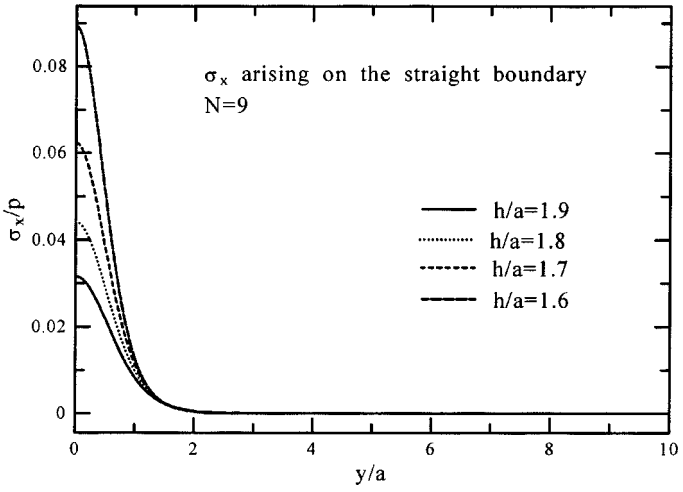

Fig. 6 Error on the straight boundary

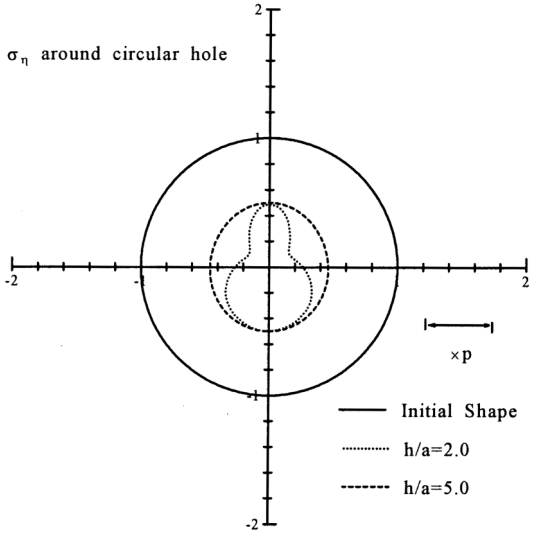

Fig. 7 Tangential stress around the hole subjected to uniform normal stress

Fig. 8. Tension appears on the top and bottom of the hole, for which the normal stress corresponds to tension, and compression appears on the side of hole, for which the normal stress corresponds to compression. The value of the tension appearing on the top of the hole is the same as that appearing on the bottom of the hole when the hole is deep. However, when the hole is shallow, the tension appearing on the top of the hole is about 1.5 times greater than that appearing on the bottom of the hole. Also the compression when the hole is shallow is larger than that when the hole is deep.

Fig. 11 shows the tangential stress around the circular hole at h/a=2.0 and 5.0 when asymmetric stress depending on the polar angle, namely on θ, $\sigma_\xi = p \cos(2\theta + \pi/4)$, is loaded on the circular hole as shown in Fig. 10. In this case, the normal stress exhibits both compression and tension. Both the tension and the compression arise on the nearest side to the straight boundary are larger than those arising on the opposite side.

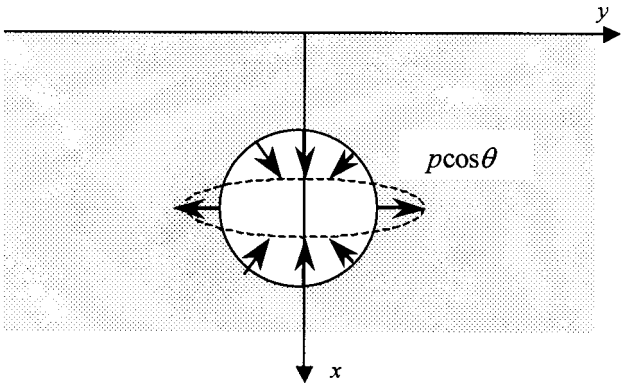

Fig. 8 Symmetric normal stress on the circular hole

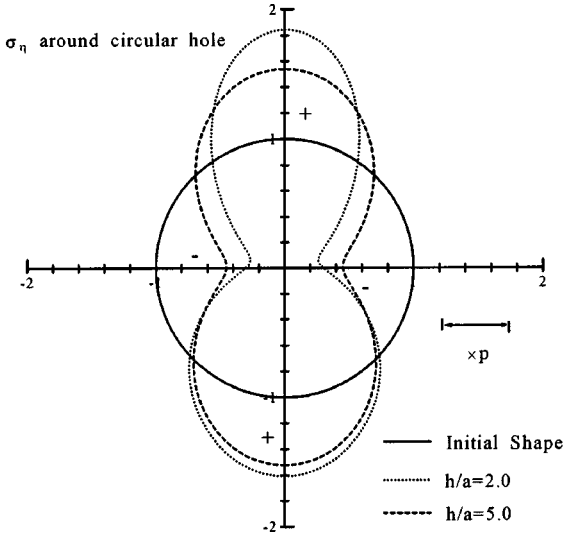

Fig. 9 Tangential stress arising on the hole subjected to symmetric normal stress

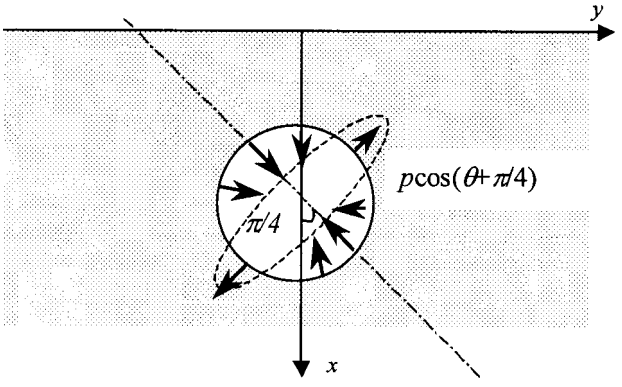

Fig. 10 Asymmetric normal stress on the circular hole

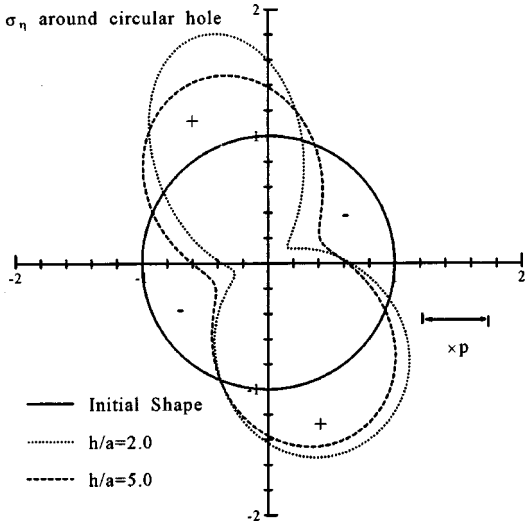

Fig. 11 Tangential stress arising around the hole subjected to asymmetric normal stress

5. Conclusions

In this paper, solutions are proposed for an isotropic elastic semi-infinite plane with a circular hole under arbitrary load on the circular hole by superposing the solutions for an isotropic elastic infinite plane with one circular hole and the solutions for an isotropic elastic semi-infinite plane until the required boundary conditions are met. Some numerical results are presented and it is shown that the semi-infinite plane containing a circular hole can be regarded as an infinite plane with a circular hole when the hole is deep. However, in these results the hole is influenced by a straight boundary when the hole is shallow.

References

Hetenyi, M. (1960), "A method of solution for the elastic quarter-plane", *J. Appl. Mech*., **27**, 289-296.
Howland, R. C. J. (1930), *Phi. Trans. Roy. Soc. London*, A, **229**, 49-86.
Jeffery, G. B., (1920), *Phi. Trans. Roy. Soc. London*, A, **221**, 265-293.
Mindlin, R. D.(1939), "Stress distribution around a tunnel", *Proc. A.S.C.E.*, **65**(4), 619-642.
Moriguchi, S. (1957a), *Two Dimensional Elasticity*, (in Japanese), Iwanami. Pub.
Tamate, O. (1957b), "The effect of a circular hole on the pure twist of an infinite strip", *J. Appl. Mech*., **24**, 115-121.
Tamate, O. (1959), "Transverse flexure of a thin plate containing two circular holes", *J. Appl. Mech.* **26**, 55-60.
Tsutsumi, T. and Hirashima, K. (1997a), "Analysis of anisotropic elliptic ring by using constraint-release technique" (in Japanese), *Trans. of JSME Seriese A*, **63**(615), 2411-2416.
Tsutsumi, T. and Hirashima, K. (2000), "Analysis of orthotropic circular disks and rings under diametrical loadings", *Struct. Eng. Mech.*, **9**(1), 37-50.
Verruijt, A. (1997b), "A complex variable solution for a deforming circular tunnel in an elastic half-plane", *Int. J. Num. Analytical Meth. Geomech.*, **21**, 77-89.